Anomalous equilibrium emittance due to chromaticity in electron storage rings

Katsunobu Oide and Haruyo Koiso
National Laboratory for High Energy Physics (KEK), Oho, Tsukuba, Ibaraki 305, Japan
(Received 4 January 1994)

An anomalous equilibrium emittance due to chromaticity of the focusing elements is predicted for electron storage rings. A simple model which describes the transverse beam distribution as a function of the longitudinal phase space is given to evaluate the anomalous emittance. The anomalous emittance can be a critical difficulty in achieving a very flat beam for high-luminosity electron-positron colliders.

PACS number(s): 41.60.Ap, 29.20.Dh, 41.85.Ew

I. INTRODUCTION

Synchrotron radiation characterizes the behavior of the beam in an electron-storage ring. Its basic effects are (i) damping of longitudinal and transverse oscillation modes, (ii) stochastic excitation of the oscillations due to the quantized nature of the radiation, and (iii) achieving equilibrium distribution determined as the balance of the processes (i) and (ii) [1]. In usual situations the momentum of the radiated photon is much smaller than the beam momentum, and also the number of photons per damping time is very high. Therefore, the equilibrium distribution is approximated by a Gaussian in the six-dimensional phase space, and thus specified by the mean value and the variance of the phase-space variables. To describe the motion of a particle in a storage ring, it is convenient to choose the position s along the reference orbit around the ring as the independent variable [2]. In this case the phase space is described by six variables $\mathbf{x}=(x,p_x,y,p_y,z,\delta)^T$, where x and y are the horizontal and vertical displacements from the reference orbit, p_x and p_y are their canonical conjugate momenta, δ is the deviation of the momentum from the reference, and z is its conjugate, respectively. As a convention we normalize p_x, p_y, and δ in units of the reference momentum p_0.

The equilibrium orbit and the variance are determined by the steady-state solution [3,4],

$$\begin{aligned}&\mathbf{x}_e=T[\mathbf{x}_e]\ ,\\&V=MVM^T+B\ ,\end{aligned}\tag{1}$$

where $\mathbf{x}_e$ is the equilibrium orbit at s, T is the one-turn transformation of the ring, and $V\equiv\langle\mathbf{u}\mathbf{u}^T\rangle=\langle(\mathbf{x}-\mathbf{x}_e)(\mathbf{x}-\mathbf{x}_e)^T\rangle$ is the variance matrix around $\mathbf{x}_e$. The one-turn transfer matrix M is evaluated around the equilibrium orbit starting at s. Both T and M include the damping by the synchrotron radiation. The matrix B represents the excitation of the oscillation by the radiation. The specific forms of M and B are determined by the electromagnetic structure of the storage ring. The solution of Eq. (1) is expressed in terms of magnetic focusing strengths and beam-optical functions in simple cases as shown in Refs. [1] and [4]. Equation (1) involves linear resonances including synchrotron-betatron coupling caused by, for example, dispersion at accelerating cavities [5]. Let us define the equilibrium emittances of the beam as the eigenvalues of the equilibrium matrix V. Although the emittances defined in such a manner depend on the location s in the ring, their differences at different s are at most in the order of (revolution period)/(damping period), which is typically 1/1000. Thus they effectively behave as invariants.

The equilibrium solution V to Eq. (1) is only consistent when T is nearly linear around $\mathbf{x}_e$, and the matrix B is almost constant within the resulting equilibrium beam size. One of the examples violating these conditions has been known [6] as so-called nonlinear wigglers, which were proposed to achieve a non-Gaussian distribution by changing B and M drastically. Another known example is applying an rf accelerating voltage with higher harmonics which distort Gaussian distribution. In this paper we will point out a general phenomenon in which the real variance significantly differs from that estimated using Eq. (1). In most storage rings the transverse transformation is almost linear in the range of a few standard deviations of the equilibrium beam size, except the beam-beam effect of colliding beams which is beyond the scope of this paper. Although the longitudinal (synchrotron) motion itself is also nearly linear, the transverse transformation can be affected by the synchrotron motion due to chromatic effects of the focusing structure of the ring. Usually the natural chromaticity of the transverse focusing force is so corrected as to have enough acceptance for the injected beam and to guarantee a long lifetime for the stored beam. The residual terms, however, may disturb the equilibrium beam size. We call the emittance produced by the chromatic effects "anomalous emittance," whereas that determined by the solution V of Eq. (1) is referred to as "linear emittance." The anomalous emittance is particularly serious for high luminosity colliders, e.g., B-meson factories, which squeeze the beam at the interaction point (IP) to increase the luminosity [7]. Some of those machines also require a very flat beam whose vertical-to-horizontal emittance ratio is as small as 1%. Therefore the chromatic effects are critical for such flat-beam machines, because they easily degrade the vertical emittance. Moreover, a colliding machine usually has a longitudinal magnetic field at the IP for the particle detector. This longitudinal field also leads to the anomalous emittance. Even if its x-y coupling effects are com-

TABLE I. Related parameters of the B-meson factory at KEK.

Beam energy	E	3.5	GeV
Transverse tunes	μ_x/μ_y	41.11/41.19	2π
Linear emittances	$\varepsilon_{x0}/\varepsilon_{y0}$	18.0/0.014	nm
Relative momentum spread	σ_δ	7.4×10^{-4}	
Circumference	cT_0	3010	m
Synchrotron damping period	τ/T_0	4150	turns
β functions at the IP	β_x^*/β_y^*	1/0.01	m
Solenoid field at the IP	$B_z l_s$	1×2.2	T m

pensated by other magnets only at the designed momentum, the remaining chromatic change of the coupling term is still big enough to blow up the vertical emittance, as shown below. This paper proposes a model to evaluate the anomalous emittance quantitatively. We also show several results by applying the model to a design of a ring for the B-meson factory at KEK as an example [8], whose parameters are listed in Table I.

II. EQUILIBRIUM DISTRIBUTION AS A FUNCTION OF LONGITUDINAL VARIABLES

First we assume that the one-turn transformation around the equilibrium orbit $\mathbf{x}_e$ is linear in the transverse direction, and that the longitudinal oscillation itself is also linear and independent of the transverse motion. Therefore, the longitudinal oscillation without radiation is a simple sinusoidal motion in the phase space around the equilibrium values δ_e and z_e,

$$\begin{aligned}\delta&=\sqrt{2J_z}\cos n\mu_z+\delta_e\ ,\\ z&=\sqrt{2J_z}\sin n\mu_z+z_e\ ,\end{aligned}\tag{2}$$

where J_z is the longitudinal action, μ_z is the phase advance of the synchrotron motion per one revolution, and $\phi_z=n\mu_z$ is the longitudinal angle at the n-th turn. The number $\mu_z/2\pi$ is often called a synchrotron tune. Note that Eq. (2) assumes a normalization of δ and z, so that the motion becomes circular in the phase space. In the present example, the final results turn out to be consistent with the assumption that the longitudinal distribution is not affected by the chromatic effects. Due to the chromatic effects of the transverse transformation, the equilibrium distribution inevitably depends on the longitudinal coordinates (J_z,ϕ_z). Although this equilibrium solution also depends on s, all variables are evaluated at a particular location s for the time being. Thus all variables are defined at s hereafter. We propose a natural generalization of the equilibrium equation (1), so that it describes the transverse distribution dependent on (J_z,ϕ_z) as well. Since the transverse motion is linear, the equilibrium distribution is still Gaussian in the transverse direction and can be specified by the variances which now depend on (J_z,ϕ_z). In what follows, we restrict our attention only on the transverse distribution and use transverse four-dimensional vectors and 4×4 matrices. We impose an additional condition that the original matrix M is separated into the transverse part U and longitudinal part. This condition is usually satisfied by choosing s at a place where the linear momentum dispersion of the transverse orbit is suppressed.

We define the mean value $\mathbf{h}$ of the orbit deviation from the transverse part of $\mathbf{x}_e$ and the transverse variance matrix W around $\mathbf{h}$ as

$$\begin{aligned}\mathbf{h}(J_z,\phi_z)&=\int(\mathbf{x}_t-\mathbf{x}_{te})f(\mathbf{x}_t,J_z,\phi_z)d\mathbf{x}_t/\rho(J_z)\ ,\\ W(J_z,\phi_z)&=\int(\mathbf{x}_t-\mathbf{x}_{te})(\mathbf{x}_t^T-\mathbf{x}_{te}^T)\\ &\quad\times f(\mathbf{x}_t,J_z,\phi_z)d\mathbf{x}_t/\rho(J_z)\ ,\end{aligned}\tag{3}$$

where f is the six-dimensional distribution function at s, and the integration is performed over the transverse phase space. The subscript t indicates the transverse part. The longitudinal distribution $\rho(J_z)$ is Gaussian, i.e.,

$$\int f(\mathbf{x}_t,J_z,\phi_z)d\mathbf{x}_t=\rho(J_z)=\exp(-J_z/\sigma_\delta^2)/\sigma_\delta^2\ ,\tag{4}$$

where σ_δ is the momentum spread. Since we have assumed that the synchrotron motion is sinusoidal, which advances the phase ϕ_z by μ_z in one revolution of the ring as Eq. (2), the equilibrium distribution satisfies these equations:

$$\begin{aligned}\mathbf{h}(J_z,\phi_z+\mu_z)&=U\mathbf{h}(J_z,\phi_z)+\mathbf{d}+\Delta\mathbf{h}\ ,\\ W(J_z,\phi_z+\mu_z)&=UW(J_z,\phi_z)U^T+\mathbf{d}\mathbf{h}^TU^T+U\mathbf{h}\mathbf{d}^T\\ &\quad+\mathbf{d}\mathbf{d}^T+D+\Delta W\ ,\end{aligned}\tag{5}$$

The right-hand side (rhs) of Eq. (5) expresses the transfer of the beam distribution in one revolution associated with the transverse one-turn map. All vectors and matrices on the rhs of Eq. (5) are evaluated at (J_z,ϕ_z). The terms $\Delta\mathbf{h}$ and ΔW represent the damping and diffusion in the longitudinal phase space described in the next paragraph. The matrix $U(J_z,\phi_z)$ now involves all chromaticities in the transverse transfer matrix including x-y coupling terms, and $\mathbf{d}(J_z,\phi_z)$ is the source of the higher-order momentum dispersion of the transverse orbit. According to our assumption on the transverse linearity, the matrix U does not depend on the amplitude of the mean value $\mathbf{h}$. The excitation matrix $D(J_z,\phi_z)$ also reflects the chromatic effects of the ring.

In addition to the transverse transfer described above, we have to take into account that both the damping and the diffusion in the longitudinal phase space also transfer the transverse beam distribution. This longitudinal transfer is described by the Fokker-Planck equation [9],

$$\left[\frac{\partial f}{\partial t}\right]_{\text{long}}=\frac{2}{\tau}\frac{\partial}{\partial\delta}\left[\delta f+\sigma_\delta^2\frac{\partial f}{\partial\delta}\right]\ ,\tag{6}$$

where τ is the longitudinal damping time. According to the definitions Eq. (3), the quantities $\rho(J_z)\mathbf{h}$ and $\rho(J_z)W$ should satisfy the same equation as Eq. (6). Since the time scale of the synchrotron motion is longer than the revolution period T_0 in most rings, we can estimate the effect simply by multiplying the rhs of (6) by T_0. This

treatment is equivalent to assuming the diffusion and the damping in the longitudinal phase space to be an impulse at the location s.

A practical way to solve Eq. (5) is to use a Fourier expansion,

$$g(J_z,\phi_z)=\sum_k \bar{g}_k(J_z)\exp(ik\phi_z) , \tag{7}$$

for all variables in Eq. (5), where the overbars stand for Fourier coefficients. Then Eq. (5) reduces to

$$\begin{aligned}\bar{\mathbf{h}}_k(J_z)\exp(ik\mu_z)&=\sum_l \bar{U}_{k-l}(J_z)\bar{\mathbf{h}}_l(J_z)\\&\quad+\bar{\mathbf{d}}_k(J_z)+\overline{\Delta\mathbf{h}}_k(J_z) ,\\ \bar{W}_k(J_z)\exp(ik\mu_z)&=\sum_l \overline{(U\otimes U^T)}_{k-l}(J_z)\bar{W}_l(J_z)\\&\quad+[\overline{\mathbf{dh}^T U^T}+\overline{U\mathbf{hd}^T}+\overline{\mathbf{dd}^T}+\bar{\mathbf{D}}]_k(J_z)\\&\quad+\overline{\Delta W}_k(J_z) .\end{aligned} \tag{8}$$

These are linear equations for $\bar{\mathbf{h}}_k(J_z)$ and $\bar{W}_k(J_z)$, including the additional terms $\overline{\Delta\mathbf{h}}_k$ and $\overline{\Delta W}_k$, expressed as

$$\begin{aligned}\overline{\Delta g}_k(J_z)=\frac{2T_0}{\tau\rho(J_z)}\Bigg[&\Delta_J\left[\bar{g}_k+\frac{(\bar{g}_{k-2}+\bar{g}_{k+2})}{2}\right]-k^2\frac{\sigma_\delta^2}{4J_z}\bar{g}_k(J_z)+\frac{k-2}{4}\left[1+\frac{k}{2J_z}\right]\bar{g}_{k-2}(J_z)-\frac{k+2}{4}\left[1-\frac{k}{2J_z}\right]\bar{g}_{k+2}(J_z)\\&-\frac{k-1}{2}\bar{g}'_{k-2}(J_z)+\frac{k+1}{2}\bar{g}'_{k+2}(J_z)\Bigg] ,\end{aligned} \tag{9}$$

where g is either $\mathbf{h}$ or W, and

$$\Delta_J(\xi)\equiv(\sigma_\delta^2-J_z)\xi'(J_z)+\sigma_\delta^2 J_z\xi''(J_z) . \tag{10}$$

Then is is feasible to solve Eq. (8) numerically, once the functions $U(J_z,\phi_z)$, $\mathbf{d}(J_z,\phi_z)$, and $D(J_z,\phi_z)$ are given.

In practice we solved Eq. (8) in the case of our example ring as follows. The functions $U(J_z,\phi_z)$, $\mathbf{d}(J_z,\phi_z)$, and $D(J_z,\phi_z)$ actually depend only on the momentum δ with good accuracy. Thus we obtained them by numerical integrations through the ring at 35 points δ_n in the range $|\delta|\le 4\sigma_\delta$, and calculated the Fourier components $\bar{U}$, $\bar{\mathbf{d}}$, and $\bar{D}$ from them. We took 36 mesh points in J_z direction, in the range $0\le 2J_z\le(4\sigma_\delta)^2$. The derivatives by J_z in Eq. (10) are replaced by finite differences. The length of the Fourier series was chosen to be 13, in the range $-6\le k\le 6$ [10]. We have also included the change of the synchrotron frequency depending on the amplitude J_z due to the nonlinearity of the rf wave form. After solving the equilibrium distribution as a function of (J_z,ϕ_z), we obtained the variance of the entire transverse distribution around the equilibrium orbit $\mathbf{x}_e$ by averaging over the longitudinal phase space as

$$\langle W\rangle=\int \bar{W}_0(J_z)\rho(J_z)dJ_z , \tag{11}$$

using the longitudinal distribution (4). We estimated the projected emittances of $\langle W\rangle$ by

$$\begin{aligned}\varepsilon_x&=\sqrt{\langle W\rangle_{11}\langle W\rangle_{22}-\langle W\rangle_{12}^2} ,\\ \varepsilon_y&=\sqrt{\langle W\rangle_{33}\langle W\rangle_{44}-\langle W\rangle_{34}^2} .\end{aligned} \tag{12}$$

Note that this estimation does not represent the entire transverse distribution since it is no longer Gaussian, specified only by (11). We have assumed that the original linear distribution V_t is diagonal in x and y directions with an appropriate coordinate transformation.

III. ANOMALOUS EMITTANCE AT RESONANCE LINES

Figure 1 shows the result of the estimation as functions of the synchrotron tune $\mu_z/2\pi$. We see several resonant peaks of the emittances corresponding to resonance lines $\mu_x\pm\mu_y\pm m\mu_z=2N\pi$, $2\mu_x\pm m\mu_z=2N\pi$, and $2\mu_y\pm m\mu_z=2N\pi$, where μ_x and μ_y are the transverse phase advances per one revolution, and m and N are integers.

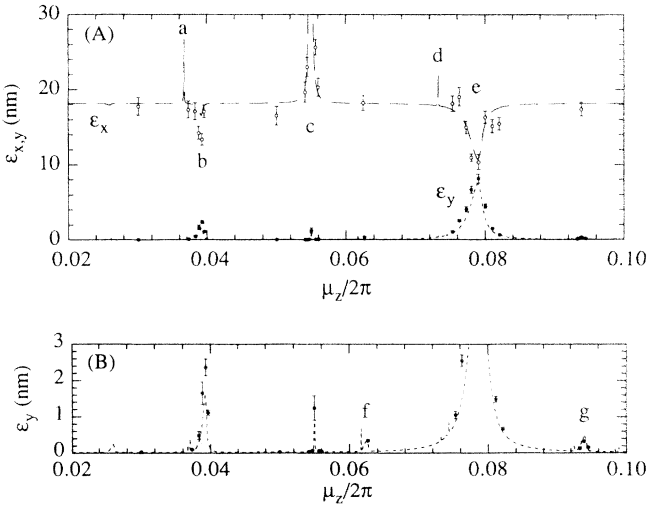

FIG. 1. The horizontal and vertical emittances as a function of the synchrotron tune. The prediction of our model (dashed and dotted curves) represents the anomalous deviation from the "linear emittances" $\varepsilon_{x0}=18.0$ nm and $\varepsilon_{y0}=0.014$ nm. These curves exhibit several resonance lines denoted as (a) $\mu_x-3\mu_z=2N\pi$, (b) $\mu_x-\mu_y+2\mu_z=2N\pi$, (c) $\mu_x-2\mu_z=2N\pi$, (d) $2\mu_x-3\mu_z=2N\pi$, (e) $\mu_x-\mu_y+\mu_z=2N\pi$, (f) $\mu_y-3\mu_z=2N\pi$, and (g) $\mu_y-2\mu_z=2N\pi$, where $\mu_x/2\pi=41.11$, $\mu_y/2\pi=41.19$, and N is an integer. The open and filled circles with error bars are the results of the particle-tracking simulation. Panel (B) magnifies the vertical scale of (A).

These resonances are possible because we have taken the nonlinearity into account only for the longitudinal variables, and have assumed transverse motion to be linear. There are mainly three kinds of sources to induce these resonances of emittances. The first one is the chromaticity of the x-y coupling term of the transfer matrix U, which excites $\mu_x \pm \mu_y \pm m\mu_z = 2N\pi$, i.e., coupling resonances. Figure 1 shows two coupling resonances (labeled b and e). The second source is the higher-order momentum dispersion in each plane which leads to $\mu_x \pm m\mu_z = 2N\pi$ and $\mu_y \pm m\mu_z = 2N\pi$ lines (denoted by a, c, f, and g). The third one is the chromaticity of the linear transformation in each plane corresponding to $2\mu_x \pm m\mu_z = 2N\pi$ and $2\mu_y \pm m\mu_z = 2N\pi$ (d in Fig. 1). A resonance line of the second type may be accompanied by the third one simultaneously. While the coupling resonance generates the off-diagonal elements in the variance matrix $W(J_z, \phi_z)$ and increases its diagonal components, the higher-order dispersion blows up the mean value $\mathbf{h}(J_z, \phi_z)$. We performed a particle-tracking simulation with a computer code SAD [7], and confirmed the result of the estimation. The tracking is based on a symplectic transformation in six-dimensional phase space for each element of the ring, and the synchrotron radiation in dipole and quadrupole magnets is taken into account. Rather than simulating the emission of each photon with the exact spectrum, we approximated the spectrum using uniform random numbers, which have the same expectation values of the energy loss and the energy fluctuation as the real photon, to save the computing time. This procedure is reasonable because the critical energy of each photon divided by the beam energy is typically 1.7×10^{-6} and the number of photons per one revolution is 450 in this ring. We tracked 20 particles during 50 000 turns starting at zero amplitude, while the radiation damping time is 4000 and 8000 turns for the longitudinal and transverse modes, respectively. We averaged the amplitudes of the particles after the 10 000th turn. The results of the tracking are depicted by circles in Fig. 1. The error bar corresponds to 1σ of the statistical error. The simulation confirms the estimation based on Eqs. (5)–(12) very well.

Beside the numerical results above, it is worth deriving an analytic solution for Eq. (8). In this paper we only show the result for the simplest case, which is the main resonance $\mu_x - \mu_y + \mu_z = 2N\pi$ (denoted by e in Fig. 1). To derive an analytic solution, we have to make several simplifications. First we assume that the transfer matrix U has its chromatic terms only in x-y coupling. The 4×4 transfer matrix U can be decomposed as [11]

$$U = \begin{pmatrix} aI & -JR^T(\delta)J \\ -R(\delta) & aI \end{pmatrix} \begin{pmatrix} X & 0 \\ 0 & Y \end{pmatrix} \begin{pmatrix} aI & JR^T(\delta)J \\ R(\delta) & aI \end{pmatrix}, \tag{13}$$

where

$$R \equiv \begin{pmatrix} r_1 & r_2 \\ r_3 & r_4 \end{pmatrix} \tag{14}$$

is the matrix to describe the x-y coupling, X and Y are 2×2 transfer matrices in each plane, and

$$I \equiv \begin{pmatrix} 1 & 0 \\ 0 & 1 \end{pmatrix}, \quad J \equiv \begin{pmatrix} 0 & 1 \\ -1 & 0 \end{pmatrix}. \tag{15}$$

The scalar parameter a satisfies $a^2 + |R| = 1$. Although the transfer matrix U in Eq. (5) includes the damping by radiation and the decomposition (13) is only valid for a stable symplectic matrix, we use the decomposition (13) to express the x-y coupling. In this case the damping is involved in each mode, i.e., matrices X and Y. This approximation is justified unless the damping rate is very high. We assume that only the matrix R above depends on the momentum deviation δ. Since the coupling matrix R is usually corrected for the design momentum, i.e., $R(0) = 0$, the main contribution comes from its first-order term $\partial R/\partial\delta$. Thus we take only the linear chromatic term of R as

$$R(\delta) = \begin{pmatrix} r_1' & r_2' \\ r_3' & r_4' \end{pmatrix} \delta = \begin{pmatrix} r_1' & r_2' \\ r_3' & r_4' \end{pmatrix} \sqrt{2J_z}\cos\phi_z \,. \tag{16}$$

The chromaticity of matrices X and Y should be small due to the regular chromaticity correction.

On evaluating Eq. (8), we also neglect other chromatic terms in $\mathbf{d}$, $\mathbf{h}$, and D. As we have limited the chromatic terms to Eq. (16), the leading terms of the chromatic effect appear in $\overline{W}_0$ and $\overline{W}_{\pm1}$. Therefore, we solve Eq. (8) only for $\overline{W}_0$ and $\overline{W}_{\pm1}$ up to the order of r'^2. After a lengthy calculation using Eqs. (13) and (16), and ignoring the Fokker-Planck terms, Eq. (8) gives a solution near a resonance $\mu_x - \mu_y + \mu_z = 2N\pi$,

$$\begin{aligned} &\varepsilon_x + \varepsilon_y = \varepsilon_{x0} \,, \\ &\varepsilon_y = \frac{w}{2w + (T_0/\tau_x + T_0/\tau_y)^2 + (\mu_x - \mu_y + \mu_z - 2N\pi)^2}\varepsilon_{x0} \,, \end{aligned} \tag{17}$$

where ε_{x0} is the linear emittance in the x plane, and the linear emittance in the y plane is assumed to be zero because of the flat-beam design. The parameters τ_x and τ_y are the radiation damping times in both planes. In Eq. (17), the strength and the width of the anomalous emittance are determined by the parameter

$$\begin{aligned} w \equiv &\{[\hat{r}_1' + \hat{r}_4' - \hat{r}_2'(\alpha_x - \alpha_y)]^2 \\ &+ [-\hat{r}_1'\alpha_y + \hat{r}_2'(1 + \alpha_x\alpha_y) - \hat{r}_3' + \hat{r}_4'\alpha_x]^2\} \\ &\times \left(1 + \frac{\tau_y}{\tau_x}\right)\sigma_\delta^2 \sin^2\frac{\mu_x - \mu_y}{2} \,, \end{aligned} \tag{18}$$

where $\hat{r}_i'$ are defined as

$$\begin{pmatrix} \hat{r}_1' & \hat{r}_2' \\ \hat{r}_3' & \hat{r}_4' \end{pmatrix} \equiv \begin{pmatrix} r_1'\sqrt{\beta_x/\beta_y} & r_2'/\sqrt{\beta_x\beta_y} \\ r_3'\sqrt{\beta_x\beta_y} & r_4'\sqrt{\beta_y/\beta_x} \end{pmatrix} \tag{19}$$

with Twiss parameters α_x, β_x, α_y, and β_y at the reference point.

The model ring has $w = 1.3 \times 10^{-5}$, which roughly explains the numerical result of the width of the resonance e in Fig. 1. In the case of an existing ring, the value of w has been small. For example, TRISTAN [12] has

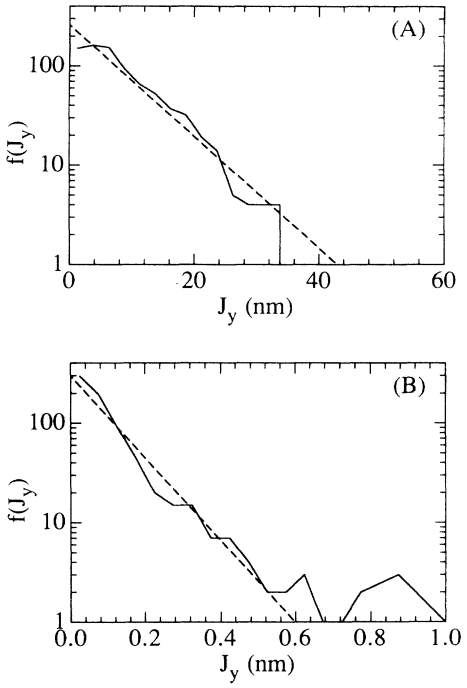

FIG. 2. Distribution of the vertical amplitude at (A) x-y coupling resonance at e, and (B) resonance of $\mathbf{h}_y$ at g. The vertical scale is in arbitrary units. The distribution (B) shows a tail in the large amplitudes, even beyond the range of the figure. The dashed line is a fitted Gaussian distribution $f(J_y) \propto \exp(-J_y/\varepsilon_{y,\mathrm{fit}})$.

$w = 5.0 \times 10^{-9}$ in the collision mode at 29 GeV. The magnitude of the parameter w depends on the relative momentum spread, the relative strength of the solenoid field at the IP, and the local chromaticity around it. Compared to the TRISTAN, the solenoid field of the model ring is factor 3 relatively stronger but its effect on w is cancelled by its smaller momentum spread ($\frac{1}{4}$ in σ_δ^2). The big difference of w comes from the chromaticity localized around the IP. A future collider like the model ring requires an extremely high local chromaticity around the IP to achieve high luminosity by strong focusing. This is the reason why the anomalous emittance has not been reported in existing machines, but can be critical for future machines.

Next we studied how the equilibrium distribution deviates from the Gaussian. We checked the distribution of the vertical amplitude by the particle tracking. Figure 2 shows the result at two resonance lines e and g in Fig. 1. While the transverse equilibrium distribution (A) at the coupling resonance e is close to the Gaussian, the distribution (B) at the resonance g has a long tail in the large amplitude region. Thus the emittance of the core, which corresponds to the slope of the fitted line in each panel of Fig. 2, is the same as the rms value at e, but $\frac{1}{3}$ at g. This

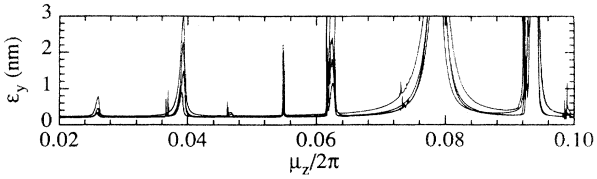

FIG. 3. Machine errors enhance the strengths of resonances of the anomalous emittance, comparing to those without errors (Fig. 1). Each trace corresponds to a different random-number seed.

difference is ascribed to the fact that at the resonance g the amplitude of the vector $\mathbf{h}$ has a sharp peak in the longitudinal phase space. On the contrary, the blow up at the resonance e is broad and limited at half the horizontal linear emittance.

It is important to evaluate the effects of machine errors on the anomalous emittance in constructing an actual machine. We estimated the effects using the model described above by putting together several kinds of random machine errors. We added 100 μm transverse offsets, 100 μrad rotation in the x-y plane, and 0.1% relative strength errors for all magnets of the example ring. We also corrected the equilibrium orbit so as to pass the center of each focusing lens within an accuracy of 100 μm. The correction scheme is a conventional one with dipole correctors. With these machine errors and the correction, the linear vertical emittance can be reduced to 1% of the horizontal one. The magnitudes of these machine errors are realistic with present technologies. Figure 3 shows the anomalous emittance for four different random-number seeds. The strengths of resonances are strongly enhanced. Therefore, the anomalous emittance we found poses a serious difficulty in achieving a very flat beam, which can be avoided only by a careful choice of the tunes (μ_x, μ_y, μ_z) and some sophisticated correction method.

IV. CONCLUSION

The model described by Eqs. (5)–(12) predicts with good accuracy the anomalous equilibrium emittance due to the chromaticity of an electron storage ring. Although the anomalous emittance degrades the performance of a very flat-beam machine with high chromaticity, it can be in principle eliminated by adding more chromatic elements, e.g., skew sextupoles at horizontally dispersive locations. Further study should be made in the case where the spread of the synchrotron frequency in a bunch or among bunches becomes big by intensity-dependent effects [13].

ACKNOWLEDGMENT

We thank K. Yokoya for helpful discussions.

[1] M. Sands, *Physics with Intersecting Storage Rings,* edited by B. Touschek (Academic, New York, 1971).
[2] E. D. Courant and H. S. Snyder, Ann. Phys. (N.Y.) **3**, 1 (1958).
[3] F. Ruggiero, E. Picasso, and L. A. Radicati, Ann. Phys. (N.Y.) **197**, 396 (1990).
[4] K. Ohmi, K. Hirata, and K. Oide, Phys. Rev. E **49**, 751 (1994).
[5] A. Piwinski, in *Proceedings of CERN Accelerator School Advanced Accelerator Physics, The Queen's College, Oxford, England, 1985, CERN 87-03,* edited by S. Turner (European Organization for Nuclear Research, Geneva, Switzerland, 1987), p. 187.
[6] J. M. Jowett, in Ref. [5], p. 570.
[7] K. Oide and H. Koiso, Phys. Rev. E **47**, 2010 (1993).
[8] *Proceedings of International Workshop on B Factories, KEK, Tsukuba, Japan, 1992,* KEK Proceedings No. 7, edited by E. Kikutani and T. Matsuda (National Laboratory for High Energy Physics, Tsukuba, Japan, 1993).
[9] J. M. Jowett, in *Physics of Particle Accelerators, Stanford Linear Accelerator Center, 1985 and Fermi National Accelerator Laboratory, 1984,* edited by Melvin Month and Margaret Dienes, AIP Conf. Proc. No. 153 (AIP, New York, 1987), p. 864.
[10] The result hardly changes, even if we increase the number to 17 in the range $-8 \leq k \leq 8$.
[11] D. A. Edwards and L. C. Teng, IEEE Trans. Nucl. Sci. **NS-20**, 885 (1973).
[12] T. Nishikawa *et al.*, KEK Report No. 86-14 (National Laboratory for High Energy Physics, Tsukuba, Japan, 1987) (unpublished).
[13] See, e.g., A. W. Chao, *Physics of Collective Beam Instabilities in High Energy Accelerators* (Wiley, New York, 1993).